Interaction Notes

Note 526

May 19, 1997

Eddy Current Responses of Canonical Metallic Targets
Theory and Measurements

Gary D. Sower

EG&G MSI

This note shows how the results of Interaction Note 499, "Low-Frequency Near-Field Magnetic Scattering from Highly, but not Perfectly, Conducting Bodies," apply to simple geometric shapes and orientations for which the magnetic polarizibility dyadic can be reduced to a scalar quantity [1,2,3]. Test data are presented which show the negative real natural frequencies (damping coefficients) of various ferrous and non-ferrous conductors, with high and low conductivity. Simple canonical shapes are used for which only a single natural resonance, or a series of resonances, is present. The shapes which are readily calculable include loops of wire and spheres.

The magnetic polarizabilities of these targets are unique, and can in principal be used as features to identify or characterize them. The magnetic polarizability of a complex object will not be the simple decay curve consisting of a few damping coefficients, but will contain all of the terms of its dyadic. The amplitude coefficients of these dyadic terms will be aspect dependant, but the values of the decay constants will be aspect independent. Thus, the determination of the decay coefficients will, in principal, uniquely determine the identity of the target object.

DEPARTMENT OF THE AIR FORCE
PHILLIPS LABORATORY (AFMC)

Date: 22 MAY 97

MEMORANDUM FOR PL/WSQW

ATTENTION: Dr. Carl E. Baum

FROM: PL/PA

SUBJECT: Phillips Laboratory Security Review Case Number(s) PL 97-0543

1. Action on the security review case mentioned above has been completed with the following determination, as marked:

X **CLEARED FOR OPEN PUBLICATION/PRESENTATION (NO CHANGES.)**

___ **CLEARED FOR OPEN PUBLICATION/PRESENTATION AS AMENDED**. The amendments, changes, deletions, etc., denoted by the words "as amended? -- are mandatory. Words of information to be deleted are indicated inside brackets.

___ **CLEARED FOR OPEN PUBLICATION/PRESENTATION WITH RECOMMENDED CHANGES.** The reviewers have suggested some changes which are not mandatory, indicated by the words "recommended changes."

___ **DISAPPROVED FOR PUBLIC RELEASE** for the following reason(s)

___ **Contained Classified Information**

___ **Contained Technology Security Information Determined Not to be releasable to the public**

___ **Release Denied for other AF/DoD/Government reasons**

X **The PL project officer must notify the author/contractor about the decision on this case and send them a copy of this letter with a copy of the stamped document (attached).**

___ **OTHER**:_____

_____.

If you have questions, please call me at (505) 846-6246.

Judy L. Johnston

JUDY L. JOHNSTON
Security Review Officer

Attachments:
PL 97-0543

Interaction Notes

Note 526

May 19, 1997

Eddy Current Responses of Canonical Metallic Targets Theory and Measurements

Gary D. Sower

EG&G MSI

This note shows how the results of Interaction Note 499, "Low-Frequency Near-Field Magnetic Scattering from Highly, but not Perfectly, Conducting Bodies," apply to simple geometric shapes and orientations for which the magnetic polarizibility dyadic can be reduced to a scalar quantity [1,2,3]. Test data are presented which show the negative real natural frequencies (damping coefficients) of various ferrous and non-ferrous conductors, with high and low conductivity. Simple canonical shapes are used for which only a single natural resonance, or a series of resonances, is present. The shapes which are readily calculable include loops of wire and spheres.

The magnetic polarizabilities of these targets are unique, and can in principal be used as features to identify or characterize them. The magnetic polarizability of a complex object will not be the simple decay curve consisting of a few damping coefficients, but will contain all of the terms of its dyadic. The amplitude coefficients of these dyadic terms will be aspect dependant, but the values of the decay constants will be aspect independent. Thus, the determination of the decay coefficients will, in principal, uniquely determine the identity of the target object.

I. INTRODUCTION

A metal detector is a device which induces eddy currents into metallic objects and then detects the magnetic fields produced by these eddy currents. A magnetic field is generated by a coil, or set of coils, through which a time-varying electrical current is driven. The frequency regime of interest is sufficiently low, a few Hertz to a few hundred kilohertz, that the targets of interest are within the near field of the illuminator. Eddy currents are induced in the conducting targets by the incident magnetic field. These currents then decay with characteristic time constants related to the resistive and inductive elements of the paths through which the induced currents flow. These impedance parameters are related to the conductivity and permeability of the metal, as well as to its geometrical shape, size and orientation, resulting in different decay patterns for different target objects. The eddy current loops then generate a secondary, scattered magnetic field which is detected by means of some magnetic field probe, usually a receiver coil which is set at a null with respect to the incident field generated by the transmitter coil.

Many metal detectors operate at a single continuous frequency (CW) which gives minimal information about the identity of the target, other than the amplitude of its magnetic moment at the particular frequency at which the system operates, and possibly the phase difference between the scattered and incident fields. Such systems can only be used for detection of metal objects. Much more information can be obtained with stepped-frequency or swept-frequency systems, or by measurements in the time domain using impulse excitation. The combination of amplitude and phase over a large frequency band contains information about the identity of the target, which can be expressed as its **magnetic polarizability** [1]. This magnetic polarizability can be characterized in the frequency domain, or equivalently (via Fourier or Laplace transforms) in the time domain.

The magnetic polarizability is the impulse response function of a metal target, that is, it is the decay response that would occur if the target were excited by a magnetic field in the form of a delta-function impulse. Of perhaps more interest is the step response of the target, as this is the response that our signal processing produces from measured data. The step response is obtained by integration of the magnetic polarizability in the time domain, or by division by the Laplace operator s in the frequency domain.

II. SIMPLIFIED PROBLEM

The scattering problem diagnosed in [1] can be simplified in computational complexity by geometries that reduce the vector and tensor quantities to scalar ones. First, let the observation direction of the scattered wave be, say, in the backward direction, toward the source (back-scatter). The radiated dipole field, the measured quantity, then reduces to:

$$\overset{\approx}{\overrightarrow{H}}^{(sc)}(\vec{r}, s) = \frac{2\,\overset{\approx}{\overrightarrow{m}}(s)}{4\pi r^3} . \qquad \text{(II.1)}$$

where the magnetic dipole moment is related to the incident magnetic field by the magnetic polarizability dyadic as:

$$\tilde{\vec{m}}(s) = \overleftrightarrow{M}(s) \cdot \tilde{\vec{H}}^{(inc)}, \qquad \text{(II.2)}$$

Then, let the scattering object have a simple shape so that it can have a magnetic moment in only a single direction. This can be done with thin conducting disks or loops which support induced eddy currents only in circular paths around the axis of symmetry. It can also be done in thin ferromagnetic rods which support induced Amperian loop currents (bound atomic or molecular currents) circulating around the axis of the rod (but in the opposite direction as would eddy currents [7]), driven by the permeability-enhanced magnetic field in the rod. The magnetic moments of these objects are aligned with their axes of symmetry.

Now let the target be aligned so that its magnetic moment (axis of symmetry) is parallel to the source and observation direction ($\vec{e}_m = \vec{e}_r$). This condition also allows for spherical target objects to be included in the discussion, because their magnetic moment is necessarily parallel to the incident field. The magnetic polarizability dyadic then reduces to a scalar value. Note that even if the alignments are not as described, only the amplitudes of the measured signals will change from the formulation presented herein.

III. CANONICAL TARGETS

The magnetic polarizability can be analytically determined for some simple objects, such as spheres and loops, which are rotationally symmetric about the axis of the magnetic moment. The simplest shape is that of a filamental loop. The filamental loop has the same response as a wire loop when the radius r of the wire is much less than the loop mean radius a [2].

1. Wire Loop: A loop of thin wire is characterized entirely by its resistance and inductance. A magnetic field incident on the loop induces a voltage around it by Faraday's law of induction. This voltage produces a current according to the impedance of the above two circuit parameters. The current defines a magnetic moment of the loop, which can be expressed as the convolution of the incident field with the magnetic polarizability of the loop in the time domain, or the product of their transforms in the frequency domain.

The magnetic polarizability is the impulse response of the wire loop. It is the eddy current decay pattern in response to an incident impulse magnetic field. The induced magnetic moment and scattered field also include the waveshape of the incident field, which we will now include. The voltage induced on the loop is determined by Faraday's law of induction around the loop of area A:

$$V(t) = \oint_C \vec{E} \cdot d\vec{\ell} = -\frac{d}{dt} \int_A \vec{B} \bullet d\vec{A} = -\vec{A} \bullet \frac{d\vec{B}}{dt} = -A\, \dot{B}(t) \cos(\theta) \,, \tag{III.1}$$

where θ is the angle between the loop axis and the incident field. The current in the loop is this voltage divided by the loop impedance, $R + sL$, which in the Laplace domain is:

$$\tilde{I}(s) = \frac{\tilde{V}(s)}{\tilde{Z}(s)} = \frac{-A\left[\, s\,\tilde{B}(s) - B(0+)\right]}{R + sL} \,, \tag{III.2}$$

where we may assume that the imposed field is initially zero:

$$B(0+) = 0 \,. \tag{III.3}$$

The magnetic dipole moment is the area of the loop times this current:

$$\tilde{m}(s) = A\,\tilde{I}(s) = -A^2 \frac{s\,\tilde{B}(s)}{R + sL} = \frac{-A^2\,\mu_0}{L} \frac{s\,\tilde{H}(s)}{\left[s + R/L\right]} \,. \tag{III.4}$$

This is equal to the product of the incident magnetic field times the magnetic polarizability of the loop, which gives the magnetic polarizability:

$$\tilde{M}(s) = \frac{-A^2\,\mu_0}{L} \frac{s\,\tilde{H}(s)}{\tilde{H}(s)\left[s + R/L\right]} = \frac{A^2\,\mu_0}{L}\left[\frac{s}{s + R/L}\right] \,. \tag{III.5}$$

In the low-frequency regime where skin effects can be ignored, typically below 100 kHz, R and L are constant. The low-frequency resistance around a <u>circular</u> wire loop is given in terms of its wire length $2\pi a$, cross-sectional area πr^2, and conductivity σ as:

$$R_0 = \frac{2\,\pi\,a}{\pi\,r^2\,\sigma} = \frac{2\,a}{r^2\,\sigma} \,. \tag{III.6}$$

At higher frequencies where the skin depth becomes smaller than the wire radius, the current becomes trapped on the wire surface within a boundary layer equivalent in depth to the skin depth. This smaller cross-sectional area increases the resistance of the wire, changing it by an expression $F_{wire\ loop}(r/\delta)$ which depends upon the ratio of the wire radius to the skin depth by the Kelvin functions, and hence the zero order Bessel function:

$$Ber(q) + jBei(q) = J_0\left(j^{-1/2} q\right) , \tag{III.7}$$

as [3]:

$$R = R_0 \frac{r}{\sqrt{2}\,\delta}\left[\frac{Ber(q)\ Bei'(q) - Bei(q)\ Ber'(q)}{\left(Ber'(q)\right)^2 + \left(Bei'(q)\right)^2} \right] = R_0\ F_{wire\ loop}(r/\delta) . \tag{III.8}$$

where the parameter q is defined in terms of the ratio of the wire radius to its skin depth:

$$q = \frac{\sqrt{2}\,r}{\delta} . \tag{III.9}$$

An empirical approximation to this skin effect, accurate to within one percent, is:

$$R = R_0 \left[1 + \left(\frac{r}{2\,\delta} + \frac{1}{4} \right)^8 \right]^{1/8} . \tag{III.10}$$

At low frequencies, this approximates R_0. At very high frequencies it becomes:

$$R = R_0 \frac{r}{2\,\delta} = \frac{a}{r} \sqrt{f\left(\frac{\pi\,\mu}{\sigma} \right)} . \tag{III.11}$$

For a <u>rectangular</u> wire loop with sides a and b, and diagonal $d=(a^2+b^2)^{1/2}$ the low-frequency resistance is:

$$R_0 = \frac{2\,(a+b)}{\pi\,r^2\,\sigma} . \tag{III.12}$$

The inductance of the <u>circular</u> loop with relative wire permeability μ_r is given to second order in (r/a) by [4]:

$$L = \mu_0\ a \left[\left(1 + \frac{r^2}{8\,a^2} \right) \ln\left(\frac{8\,a}{r} \right) + \frac{r^2}{24\,a^2} - 2 + \frac{\mu_r}{4} \right] . \tag{III.13}$$

For $r \ll a$ in non-permeable conductors (μ_r=1), this reduces to:

$$L \approx \mu_0 \, a \left[\ln\left(\frac{8\,a}{r}\right) - 1.75 \right] \equiv a\,\mu_0\, G_{wire\ loop}(a/r) \ . \qquad \text{(III.14)}$$

A frequency-independent, dimensionless variable $G_{wire\ loop}(a/r)$ is defined which contains the ratio of the loop-to-wire diameters, but is rather insensitive to this ratio because it is only within a logarithmic term.

For the rectangular loop it is given by [4]:

$$L = \frac{\mu_0}{\pi}\left[a \ln\left(\frac{2\,a\,b}{r\,(a+d)}\right) + b \ln\left(\frac{2\,a\,b}{r\,(b+d)}\right) + 2\,d - \left(2 - \frac{\mu_r}{4}\right)(a+b) \right] . \qquad \text{(III.15)}$$

which can also be defined in terms of a variable $G_{wire\ loop}(a/r)$, but not in such a simple form as for the circular loop.

In the low-frequency approximation, the resistance and inductance determine a single exponential time constant:

$$\tau_{wire\ loop} = \frac{L}{R} = \frac{r^2\,\sigma\,\mu_0}{2}\, G_{wire\ loop}(a/r) \ . \qquad \text{(III.16)}$$

The magnetic polarizability is then:

$$\tilde{M}(s) = \frac{(\pi\,a^2)^2\,\mu_0}{a\,\mu_0\, G_{wire\ loop}(a/r)}\left[\frac{s}{s + 1/\tau_{wire\ loop}}\right] = M_0\left[-1 + \frac{1/\tau_{wire\ loop}}{s + 1/\tau_{wire\ loop}}\right] . \qquad \text{(III.17)}$$

with amplitude:

$$M_0 = \frac{\pi^2\,a^3}{G_{wire\ loop}(a/r)} \ . \qquad \text{(III.18)}$$

This amplitude is, to first order in small loop size-to-source distance, proportional to the cubic power of the loop radius, and varies only slightly with the wire size. The time constant is proportional to the square of the wire radius (and to the conductivity), and varies only slightly with the loop size. The two radii which characterize the loop thus determine two distinct and separate properties of the eddy current response.

The time domain representation of the magnetic polarizability of the wire loop in the low-frequency regime can now be given in terms of the time constant of (III.16) as:

$$M(t) = M_0 \left[-\delta(t) + \frac{1}{\tau_{wire\ loop}} e^{-t/\tau_{wire\ loop}} u(t) \right] . \qquad \text{(III.19)}$$

The step response of the magnetic polarizability is:

$$\tilde{S}(s) = \frac{1}{s} \tilde{M}(s) = M_0 \left[\frac{1}{s + 1/\tau_{wire\ loop}} \right] , \qquad \text{(III.20)}$$

$$S(t) = \int_{-\infty}^{t} M(t') \, dt' = -M_0 \, e^{-t/\tau_{wire\ loop}} \, u(t) . \qquad \text{(III.21)}$$

The units of the magnetic polarizability are (m^3/s). The step response has units of (m^3).

2. Two Coaxial Loops: The effect of the mutual inductances of multiple filamental loops within an object can be illustrated the simple case of two circular coaxial wire loops. One of the loops has a radius of a_1 and wire radius r_1, the other loop a_2 and wire radius r_2. With a separation between the loops of b. The resistance and inductance of each loop are obtained from the expressions in the preceding section, giving values of R_1 and L_1. The resistance of the system may be written in matrix form as:

$$(R) = \begin{pmatrix} R_1 & 0 \\ 0 & R_2 \end{pmatrix} . \qquad \text{(III.22)}$$

The mutual inductance between the two loops is [4]:

$$M = \frac{2\,\mu_0}{k} \sqrt{a_1 a_2} \, \left[K(k) - E(k) \right] , \qquad \text{(III.23)}$$

where E(k) and K(k) are the complete elliptic integrals and the variable k is given in terms of the minimum and maximum diagonals, d_1 and d_2, between the loops:

$$k = \sqrt{\frac{d_2 - d_1}{d_2 + d_1}} . \qquad \text{(III.24)}$$

The total inductance of the system may then be written in matrix form as:

$$(L) = \begin{pmatrix} L_1 & M \\ M & L_2 \end{pmatrix} . \qquad \text{(III.25)}$$

An impedance matrix can now be constructed:

$$(Z) = (R + sL) = \begin{pmatrix} R_1 + sL_1 & sM \\ sM & R_2 + sL_2 \end{pmatrix} . \qquad \text{(III.26)}$$

A voltage is induced onto each loop from the incident magnetic field by Faraday's law, which can be written in vector form, with an angle θ between the loop axes and the incident field:

$$(V(t)) = \begin{pmatrix} -A_1 \dot{B}(t) \cos(\theta) \\ -A_2 \dot{B}(t) \cos(\theta) \end{pmatrix} = -\dot{B}(t) \cos(\theta) \begin{pmatrix} A_1 \\ A_2 \end{pmatrix} , \qquad \text{(III.27)}$$

$$(V(s)) = -s \tilde{B}(s) \cos(\theta) \begin{pmatrix} A_1 \\ A_2 \end{pmatrix} . \qquad \text{(III.28)}$$

This voltage is related to the currents on the loops by the matrix form of Ohm's law:

$$(V) = (I)(Z) . \qquad \text{(III.29)}$$

The currents can be obtained by inverting the equation:

$$(I) = (V)(Z)^{-1} , \qquad \text{(III.30)}$$

Where the inverse of the impedance matrix is:

$$(Z)^{-1} = \frac{1}{(R_1 + sL_1)(R_2 + sL_2) - (sM)^2} \begin{pmatrix} R_2 + sL_2 & -sM \\ -sM & R_1 + sL_1 \end{pmatrix} . \qquad \text{(III.31)}$$

The currents in the two loops are then:

$$(I) = \begin{pmatrix} I_1 \\ I_2 \end{pmatrix} = \frac{-s\,\tilde{B}(s)\,\cos(\theta)}{(R_1 + s L_1)(R_2 + s L_2) - (s M)^2} \begin{pmatrix} A_1\,[R_2 + s L_2 - s M] \\ A_2\,[R_1 + s L_1 - s M] \end{pmatrix} . \qquad \text{(III.32)}$$

The resonances are given by the singularities of this expression, the roots of which occur when the denominator is zero:

$$(R_1 + s L_1)(R_2 + s L_2) - (s M)^2 = 0 . \qquad \text{(III.33)}$$

One root is associated with each loop:

$$s_1 = \frac{-R_1}{(L_1 + M)} , \qquad s_2 = \frac{-R_2}{(L_2 + M)} . \qquad \text{(III.34)}$$

The magnetic dipole moment is given by:

$$\tilde{m}(s) = \sum A\,I = -\frac{s\,\mu_0\,\tilde{H}(s)\,\cos(\theta)\,A_1^2}{R_1 + s(L_1 + M)} - \frac{s\,\mu_0\,\tilde{H}(s)\,\cos(\theta)\,A_2^2}{R_2 + s(L_2 + M)} . \qquad \text{(III.35)}$$

The magnetic polarizability is thus:

$$\tilde{M}(s) = \frac{\tilde{m}(s)}{\tilde{H}(s)} = -\mu_0\,\cos(\theta) \left(\frac{s\,A_1^2}{R_1 + s(L_1 + M)} + \frac{s\,A_2^2}{R_2 + s(L_2 + M)} \right), \qquad \text{(III.36)}$$

or:

$$\tilde{M}(s) = -\mu_0\,\cos(\theta) \left[\frac{A_1^2}{L_1 + M} \left(\frac{s}{s + \frac{R_1}{L_1 + M}} \right) + \frac{A_2^2}{L_2 + M} \left(\frac{s}{s + \frac{R_2}{L_2 + M}} \right) \right]. \qquad \text{(III.37)}$$

Each loop has a <u>single</u> decay time constant, different for each loop, giving the decay response of the magnetic polarizability as:

$$M(t) = \frac{A_1^2 \mu_0 \cos(\theta)}{L_1 + M}\left[-\delta(t) + \frac{1}{\tau_1} e^{-t/\tau_1} u(t)\right] + \frac{A_2^2 \mu_0 \cos(\theta)}{L_2 + M}\left[-\delta(t) + \frac{1}{\tau_2} e^{-t/\tau_2} u(t)\right]. \quad \text{(III.38)}$$

The step response is then:

$$S(t) = -\frac{A_1^2 \mu_0 \cos(\theta)}{L_1 + M}\left[e^{-t/\tau_1} u(t)\right] - \frac{A_2^2 \mu_0 \cos(\theta)}{L_2 + M}\left[e^{-t/\tau_2} u(t)\right]. \quad \text{(III.39)}$$

When the two loops are identical in size and wire size, the areas, resistances and self inductances are the same and the decay response has only a single time constant:

$$S(t) = -\frac{2 A^2 \mu_0 \cos(\theta)}{L + M}\left[e^{-t/\tau_{dual\ wire\ loops}} u(t)\right]. \quad \text{(III.40)}$$

The magnitude of both L and M are proportional to the loop radius a, so that M_0 is proportional to a^3 as for the case of the single loop.

This example can conceptually be extended to a very large number of loops, which in the limit can form solid bodies of any shape. When the loops are all of the same size, such as for the following example of the cylindrical loop, then we expect the magnetic polarizability to have a single decay time constant. When they are of different size, such as in a thin disk or a solid sphere, we would expect to observe an infinite series of time constants.

3. Thin Cylindrical Loop: When the axis of a thin-walled cylindrical loop of radius *a,* length *b,* and wall thickness *d* is orientated so that it is parallel to the incident magnetic field, only those fields that are inscribed by the loop can induce currents on it by Faraday's law of induction, so that currents are induced only on the inner surface of the wall. The results presented in Reference [3], page 301 then apply, giving the total resistance around the loop to be:

$$R = R_0 \frac{d}{\delta}\left[\frac{\sinh(2\,d/\delta) + \sin(2\,d/\delta)}{\cosh(2\,d/\delta) - \cos(2\,d/\delta)}\right] \equiv R_0\, F_{cyl.\ loop}(d/\delta)\ , \quad \text{(III.41)}$$

where a new resistive function of wall thickness and skin depth has been defined. The low frequency resistance *(δ » d)* is:

$$R_0 = \frac{2\,\pi\,a}{b\,d\,\sigma}\ . \quad \text{(III.42)}$$

The inductance of the loop is given in Reference [4], page 5-31:

$$L = \frac{\mu_0 a}{3}\left\{\sqrt{4 + \frac{b^2}{a^2}}\left[\left(4\frac{a^2}{b^2} - 1\right)E(k) + K(k)\right] - 8\frac{a^2}{b^2}\right\}, \qquad \text{(III.43)}$$

with the dimensionless variational parameter given by:

$$k = \frac{2a}{\sqrt{4a^2 + b^2}}, \qquad m = k^2 = \frac{diameter^2}{diameter^2 + length^2}. \qquad \text{(III.44)}$$

E(k) and *K(k)* are the complete elliptic integrals. This inductance can be defined in terms of a permeability variable that is a function of the radius and length of the loop:

$$L = a\,\mu_0\,C_{cyl.\ loop}(a/b), \qquad \text{(III.45)}$$

where:

$$C_{cyl.\ loop}(a/b) = \frac{1}{3}\left\{\sqrt{4 + \frac{b^2}{a^2}}\left[\left(4\frac{a^2}{b^2} - 1\right)E(k) + K(k)\right] - 8\frac{a^2}{b^2}\right\}. \qquad \text{(III.46)}$$

In terms of the alternate parameter *m* this is:

$$C_{cyl.\ loop}(a/b) = \frac{1}{3}\left\{\frac{2}{\sqrt{m}}\left[K(m) + \left(\frac{2m - 1}{1 - m}\right)E(m)\right] - \frac{2m}{1 - m}\right\}. \qquad \text{(III.47)}$$

This expression satisfies the condition $C_{cyl.\ loop}(a/b) = 1$ at $m \approx 0.444$ where the length-to-diameter ratio is about 1.12. For very short cylinders *(b « a)* it reduces to:

$$C_{cyl.\ loop}(a/b) \approx 2\ln\left(\frac{8a}{b}\right). \qquad \text{(III.48)}$$

For very long cylinders *(b » a)* it is:

$$C_{cyl.\ loop}(a/b) \approx \pi\frac{a}{b}. \qquad \text{(III.49)}$$

An empirical relationship for this function, valid to a few percent accuracy for lengths greater than one-fourth the diameter, is:

$$C_{cyl.\ loop}(a/b) \approx \left(0.311\frac{b}{a} + 0.305\right)^{-1}. \qquad \text{(III.50)}$$

The *single* characteristic time constant for the loop then becomes:

$$\tau_{cyl.\ loop} = \frac{L}{R} = \left(\frac{b\, d\, \mu_0\, \sigma}{2\, \pi} \right) \frac{C_{cyl.\ loop}(a/b)}{F_{cyl.\ loop}(d/\delta)} \ . \qquad \text{(III.51)}$$

Notice that this time constant is, to first order, proportional only to the thickness and length of the loop as the cross-section of the conductor (as for the wire loop), and not to its radius. The magnetic polarizability of the cylindrical loop is them given by the same form as that for the wire loop:

$$\tilde{M}(s) = \frac{A^2\, \mu_0}{L} \left[\frac{s}{s + R/L} \right] = M_0 \left[-1 + \frac{1/\tau_{cyl.\ loop}}{s + 1/\tau_{cyl.\ loop}} \right] . \qquad \text{(III.52)}$$

The time domain representation of the magnetic polarizability of the cylindrical loop can now be given by:

$$M(t) \approx M_0 \left[-\delta(t) + \frac{1}{\tau_{cyl.\ loop}}\, e^{-t/\tau_{cyl.\ loop}}\, u(t) \right] , \qquad \text{(III.53)}$$

$$S(t) \approx -M_0\, e^{-t/\tau_{cyl.\ loop}}\, u(t) \ , \qquad \text{(III.54)}$$

with:

$$M_0 = \frac{\pi^2\, a^3}{\mu_{cyl.\ loop}(a/b)} \ , \qquad \text{(III.55)}$$

and:

$$\tau_{cyl.\ loop} = \frac{b\, d\, \sigma}{2\, \pi}\, \mu_{cyl.\ loop}(a/b) \ . \qquad \text{(III.56)}$$

4. Sphere: Smythe [5] derives the eddy currents of a conducting sphere of radius a, conductivity σ, and permeability μ placed in an incident magnetic field $B_0\, e^{j\omega t}$. At a frequency ω, the magnetic dipole moment $m = \pi\, a^2\, I(\omega)$ is identical to that from a loop of radius a with a current $I(\omega)\, e^{j\omega t}$, where:

$$I(\omega) = I_0 \left[\frac{(2\mu + \mu_0)\, \nu\, I_{-1/2}(\nu) - [\mu_0(1 + \nu^2) + 2\mu]\, I_{1/2}(\nu)}{(\mu - \mu_0)\, \nu\, I_{-1/2}(\nu) + [\mu_0(1 + \nu^2) - \mu]\, I_{1/2}(\nu)} \right] , \qquad \text{(III.57)}$$

and

$$I_0 = 2\,\frac{B_0\,a}{\mu_0}, \qquad \nu = (1+j)\,\frac{a}{\delta}, \qquad \nu^2 = j\,\frac{2\,a^2}{\delta^2}, \qquad \delta = \sqrt{\frac{2}{\omega\,\sigma\,\mu}},$$

$$I_{-1/2}(\nu) = \sqrt{\frac{2}{\pi\,\nu}}\,\cosh(\nu), \qquad I_{1/2}(\nu) = \sqrt{\frac{2}{\pi\,\nu}}\,\sinh(\nu).$$

The non-integral modified Bessel functions are given here in terms of hyperbolic functions. This equation, with:

$$\nu = (1+j)\,\frac{a}{\delta} = a\,(1+j)\sqrt{\frac{\omega\,\mu\,\sigma}{2}} = a\,\sqrt{j\,\omega\,\mu\,\sigma} = a\,\sqrt{s\,\mu\,\sigma}\,, \tag{III.58}$$

becomes [1, E.12], from which we extract the natural complex frequencies (poles). These poles occur at those complex frequencies where the denominator of (III.57) is zero.

Appendix E of [1] addresses the problem for quasi-magnetostatic scattering from a highly conductive, high permeability sphere. This is valid for the condition that:

$$\sqrt{\mu_r(\omega)} \ll \sqrt{1 + \frac{\sigma}{j\,\omega\,\epsilon_0}}\,. \tag{III.59}$$

This is true for all metals at frequencies below 100 GHZ, for all relative permeabilities below 100,000 and conductivities greater than 10^5 S.

The solution for the magnetic polarizability is given [1, E.12] in terms of the relative permeability $\mu_r = \mu/\mu_0$:

$$\tilde{M}(s) = M(0) + 2\,\pi\,a^3 \left\{ \frac{(2\,\mu_r + 1)\,[\,\xi\coth(\xi) - 1\,] - \xi^2}{(\mu_r - 1)\,[\,\xi\coth(\xi) - 1\,] + \xi^2} \right\}, \tag{III.60}$$

where the first term is the low frequency limit (6E.9):

$$M(0) = 4\,\pi\,a^3\,\frac{(\mu_r - 1)}{(\mu_r + 2)}\,, \tag{III.61}$$

and inside the sphere:

$$\xi = a\sqrt{s\,\mu\,\sigma}\ , \tag{III.62}$$

is Smythe's variable v in the Laplace domain. The poles of this equation occur for those values of ξ, designated ξ_α, which give a value of zero for the denominator of (III.60). These roots are the solutions of the transcendental equation, which are dependant on only the permeability as a parameter:

$$\coth(\xi_\alpha) = \frac{1}{\xi_\alpha} - \frac{\xi_\alpha}{\mu_r - 1}\ . \tag{III.63}$$

This has all imaginary roots ξ_α, giving the negative real natural frequencies:

$$s_\alpha = \frac{\xi_\alpha^2}{a^2\,\mu\,\sigma} < 0 \quad for\ all\ \alpha\ . \tag{III.64}$$

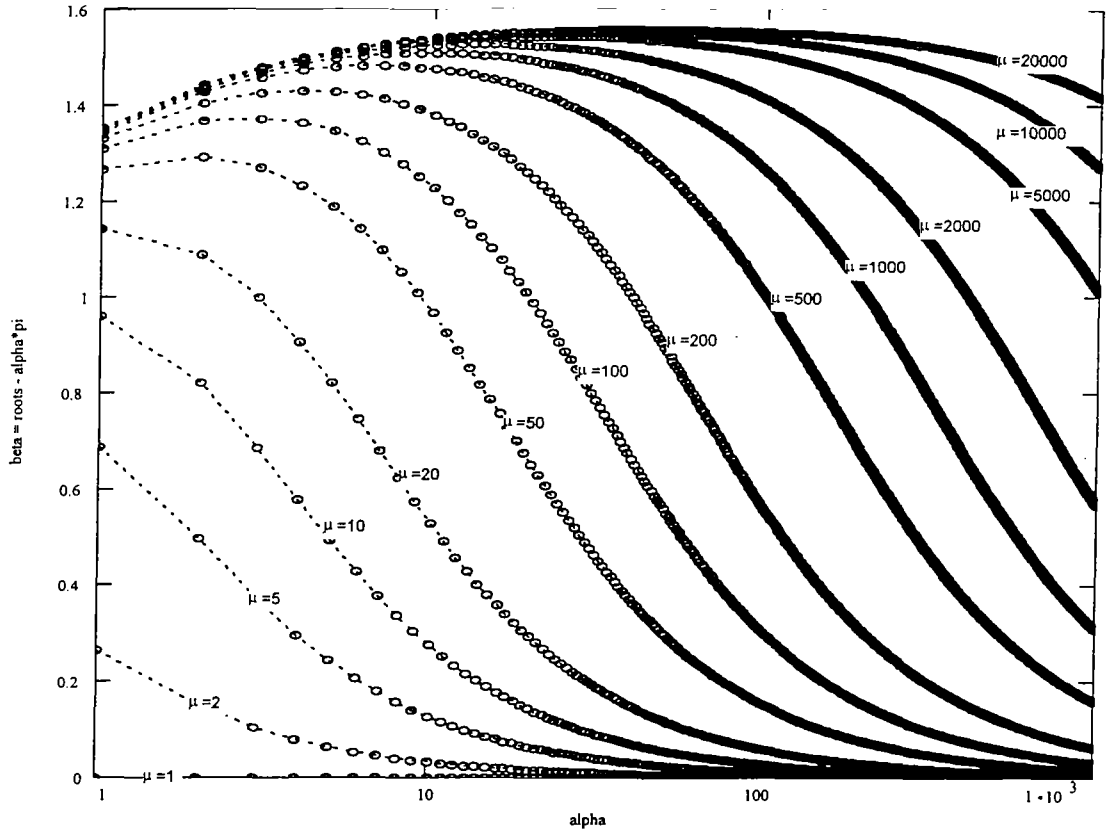

Figure 8.1. Roots of the Permeable Sphere.

The positive real time constants are then:

$$\tau_\alpha = \frac{1}{-s_\alpha} = -\frac{a^2 \mu \sigma}{\xi_\alpha^2} > 0 \quad \textit{for all } \alpha \; . \tag{III.65}$$

These roots are of the form $j\xi_\alpha = \alpha\pi + \beta_\alpha$ where $0 \le \beta_\alpha \le \frac{\pi}{2}$ as shown in Figure 8.1.

The integral of the magnetic polarizability is:

$$\widetilde{S}(s) = \frac{\widetilde{M}(s)}{s} = \frac{M(0)}{s} + \frac{2\pi a^3}{s}\left\{\frac{(2\mu_r + 1)[\xi\coth(\xi) - 1] - \xi^2}{(\mu_r - 1)[\xi\coth(\xi) - 1] + \xi^2}\right\} . \tag{III.66}$$

The step response function is given by the inverse Laplace transform of this magnetic polarizability:

$$S(t) = \frac{1}{2\pi i}\int_{c-i\infty}^{c+i\infty} e^{st}\,\widetilde{S}(s)\,d(s) \; . \tag{III.67}$$

This gives:

$$S(t) = M(0) + \frac{1}{2\pi i}\int_{c-i\infty}^{c+i\infty} \frac{2\pi a^3}{s}\left\{\frac{(2\mu_r + 1)[\xi\coth(\xi) - 1] - \xi^2}{(\mu_r - 1)[\xi\coth(\xi) - 1] + \xi^2}\right\} e^{st}\,d(s) \; . \tag{III.68}$$

The function inside the integral can be represented by the ratio of two analytic functions:

$$F(s) = \frac{f_1(s)}{f_2(s)} \; . \tag{III.69}$$

When the denominator vanishes at $s = s_\alpha$, but $f_1(s_\alpha) \neq 0$ and $f_2'(s_\alpha) \neq 0$, the Laurent expansion of $F(s)$ at $s = s_\alpha$ gives the sum of the residues:

$$\frac{1}{2\pi i}\oint \widetilde{S}(s)\,ds = \sum_{\alpha=1}^{\infty} \frac{f_1(s_\alpha)}{f_2'(s_\alpha)} \; . \tag{III.70}$$

The step response function in the time domain thus is given by:

$$S(t) = M(0) + \sum_{\alpha=1}^{\infty} 2\,\pi\,a^3 \frac{(2\,\mu_r + 1)\,[\,\xi_\alpha \coth(\xi_\alpha) - 1\,] - \xi_\alpha^2}{\frac{d}{ds}\left\{ s\left[(\mu_r - 1)\,[\,\xi \coth(\xi) - 1\,] + \xi^2 \right] \right\}_{\substack{s=s_\alpha \\ \xi=\xi_\alpha}}} e^{s_\alpha t}\,u(t) \quad . \tag{III.71}$$

Evaluation of the derivative in the denominator gives:

$$(\mu_r - 1)\,[\,\xi_\alpha \coth(\xi_\alpha) - 1\,] + \xi_\alpha^2 + s\,\xi_\alpha' \left[(\mu_r - 1)\left(\coth(\xi_\alpha) + \xi_\alpha \left[1 - \coth^2(\xi_\alpha) \right] \right) + 2\,\xi_\alpha \right]. \tag{III.72}$$

Using (III.63), and its alternative form:

$$\xi_\alpha \coth(\xi_\alpha) - 1 = \frac{-\,\xi_\alpha^2}{\mu_r - 1}\,, \tag{III.73}$$

this becomes:

$$(\mu_r - 1)\left[\frac{\xi_\alpha^2}{\mu_r - 1} \right] + \xi_\alpha^2 + s\,\xi_\alpha' \left[(\mu_r - 1)\left(\frac{1}{\xi_\alpha} - \frac{\xi_\alpha}{\mu_r - 1} + \xi_\alpha \left[1 - \left(\frac{1}{\xi_\alpha} - \frac{\xi_\alpha}{\mu_r - 1} \right)^2 \right] \right) + 2\,\xi_\alpha \right]. \tag{III.74}$$

With the evaluation of the differential:

$$\xi_\alpha' = \left(\frac{d\xi}{ds} \right)_{s=s_\alpha} = \frac{\xi_\alpha}{2\,s_\alpha}\,. \tag{III.75}$$

the denominator reduces to:

$$\frac{\xi_\alpha^2}{2}\left((\mu_r + 2) - \frac{\xi_\alpha^2}{(\mu_r - 1)} \right). \tag{III.76}$$

The step response function in the time domain thus simplifies to:

$$S(t) = M(0) - 2\,\pi\,a^3 \sum_{\alpha=1}^{\infty} \frac{6\,\mu_r\,e^{s_\alpha t}}{(\mu_r + 2)\,(\mu_r - 1) - \xi_\alpha^2}\,u(t) \quad . \tag{III.77}$$

In terms of the positive real decay time constants $\tau_\alpha = -1/s_\alpha$ this results in:

$$S(t) = 2\pi a^3 \left\{ 2\frac{(\mu_r - 1)}{(\mu_r + 2)} - \sum_{\alpha=1}^{\infty} \frac{6\mu_r e^{-t/\tau_\alpha}}{(\mu_r + 2)(\mu_r - 1) + (\alpha\pi + \beta_\alpha)^2} u(t) \right\}. \qquad \text{(III.78)}$$

The roots of the transcendental equation give the time constants:

$$\tau_\alpha = \frac{a^2 \mu \sigma}{(\alpha\pi + \beta_\alpha)^2} . \qquad \text{(III.79)}$$

The magnetic polarizability is derived in a like manner, giving:

$$M(t) = 2\pi a^3 \left\{ -\delta(t) + \sum_{\alpha=1}^{\infty} \frac{6\mu_r e^{-t/\tau_\alpha}}{(\mu_r + 2)(\mu_r - 1) + \mu\sigma a^2} u(t) \right\}. \qquad \text{(III.80)}$$

These results are based on the assumption that the permeability of the sphere is a constant value, which requires that the incident magnetic field at the target is less than about 1 A/m. This assumption is violated for all practical metal detector systems which drive a transmitter current of a few amperes through a coil of many turns and a target range of less than a meter. It is easy to excite the target with a field strength of 80 A/m, which is at the maximum of the permeability curve for commercial iron and steel, with a relative permeability reached of about 5000 as compared to about 200 at very low fields. With a transient excitation, the permeability may increase by a factor of 25 *during the time that the transient field is increasing in strength.* The permeability of ferrous objects is also frequency dependant, decreasing above 1 kHz to the free-space value at about 300 kHz [6].

If one knew the magnetic field strength at the sphere as a function of time, and knew the relative permeability as a function of the field strength, then a Fourier or Laplace transform could be taken to give the relative permeability of the sphere as a function of frequency. This could then be used in (III.60) to find the roots, with the natural frequencies of (III.64). These roots would then give the magnetic polarizability in the frequency domain from (III.77), from which an inverse transformation (IFFT) would give the time domain response.

Non-ferrous sphere: The limiting case when the permeability is exactly unity is treated by setting $\mu_r = 1$ in (III.76), which results in:

$$S(t) = -12\pi a^3 \sum_{\alpha=1}^{\infty} \frac{e^{-t/\tau_\alpha}}{n^2\pi^2} u(t) . \qquad \text{(III.81)}$$

The roots in this case are simply $n\,\pi$, giving the time constants as a simple geometric sequence:

$$\tau_n = \frac{a^2 \mu \sigma}{n^2 \pi^2} . \qquad \text{(III.82)}$$

5. Summary: The solutions for the canonical cases derived above for electrically thin non-ferrous conductors possessing a single conductor loop radius all reduce to the same generic form with a single time constant:

$$M(t) = M_0 \left[-\delta(t) + \frac{1}{\tau} e^{-t/\tau} u(t) \right] . \qquad \text{(III.83)}$$

$$S(t) = -M_0 e^{-t/\tau} u(t) . \qquad \text{(III.84)}$$

The solution for the non-ferrous solid sphere is a bit more complicated, (III.78), with an infinite number of time constants, only a finite number are within any physically realizable bandwidth, and which decrease quadratically with frequency. The solutions for other simple solid canonical shapes, such as solid cylinders, will resemble this form, as will those for electrically thin shapes of variable filamental loop radius such as thin disks and spherical shells.

The magnitude of the polarizability is proportional to the cube of the radius of the loop, disk, or sphere. The time constants are proportional to the square of the loop radius times the metal conductivity and permeability. It is thus physically impossible to distinguish between different non-ferrous metals (gold from copper for example), as claimed for many metal detectors. A small change in target size more than compensates for different conductivities. It is, however, very possible to distinguish between specific objects of known geometry and composition because the time constants can be characterized. Also, ferrous objects are readily distinguished because of the polarity change of the decay curves.

IV. MEASUREMENTS

An impulse metal detector has been used to measure the step response functions of certain canonical metal objects. The step response of the metal detector has been characterized, and this response deconvolved from the measured data to give the results presented. A Helmholtz coil is used to generate a nearly uniform field incident magnetic field. A current source is used which generates a step with a transition time of approximately 30 microseconds. A quadrupole receive coil is located to one side of the Helmholtz coil, oriented so that it is sensitive to the dipole field radiated from the target objects while giving a null response to the incident Helmholtz field. The receiver amplifier has a high-gain differential amplifier with a filtered high-frequency response. The signals are digitized with a 12 bit analog-to-digital PCA card in a portable Pentium computer. The data are acquired using Labview© control, and processed with Matlab©.

The absolute amplitudes of the measured data and the theory cannot be directly compared because of the various distance terms (*eg*, $1/r^3$) in the incident field and scattered field equations. The scattered flux intercepted by the receiver coils, signal conditioning, and amplifier gain also introduce non-calibrated variables into the amplitudes. If the data are acquired with all of these variables fixed, so that the relative amplitudes are all consistent, then a single scale constant can be used to compare the theory with experiment for all of the data sets.

The data were acquired with all of the hardware parameters fixed, except for the location of the target objects in the Helmholtz coil. The various size of the targets results in signal amplitudes which can exceed the dynamic range of the electronics if they are all located at one location with respect to the receiver coils. Therefore, the smaller objects were located closer to the receiver and the larger ones farther away, while still remaining within the constant field volume of the Helmholtz coil. The amplitude scale factors between these constant locations were measured with a given object, and then used to scale the results to a common factor. The scale factor was determined to be approximately $1/r^2$ from the receiver coil.

The deconvolution process is not perfect. The first few points of the responses show the effect of the circular FFT, distorting the exponential decay. The late-time response exhibits noise, and also shows effects of distortion of the first few frequency points.

1. Wire Loops: The measured deconvolved responses of some 5 cm diameter wire loops of American Wire Gauge (AWG) copper magnet wire are shown on Figure 8.2, along with the (dashed) theoretical waveforms from (III.20). Dual data traces are due to measurements taken at different target locations, and show the repeatability of the data. Both linear and logarithmic amplitude scales are presented. The largest wire (#12 AWG) has the largest decay time, the upper curve. The listed value of the conductivity of pure copper, 5.80×10^7 S/m, is used for the theoretical curves.

Figure 8.3 shows the responses of 10cm diameter wire loops and the theoretical curves. Notice that the time constants for each wire size are nearly the same as they are for the 5 cm loops, in agreement with (III.16). The amplitudes are a factor of eight larger, in agreement with (III.18). The smaller wire sizes exhibit more noise because of their smaller signal strength.

The agreement between measurement and theory is extremely good for the wire loops: the amplitude is proportional to the cubic power of the loop radius, and varies only slightly with the wire size. The time constant is proportional to the square of the wire radius (and to the conductivity), and varies only slightly with the loop size. The two radii which characterize the loop thus determine two distinct and separate properties of the eddy current response.

2. Coaxial Wire Loops: Figure 8.4 illustrates the response of two coaxial loops of copper magnet wire, a 5 cm diameter circular loop of No. 12 AWG and a 10 cm loop of No. 18 AWG. The responses of the two loops by themselves are also shown as the lower curves (straight lines on the logarithmic plot). The theoretical responses, the dashed lines, are included, (III.39) for the dual loops. The dual loop data deviate from theory at late time, a result of inaccuracy in the deconvolution process. The dotted line is the sum of the theoretical responses of the two individual loops, which is seen to not be the response of the system, validating (III.39).

3. Thin (Hollow) Cylindrical Loops: Hollow, thin-walled, cylindrical loops are shown by (III.54) to have a single decay time constant when the incident magnetic field is parallel to the loop axis. This is verified by the measured data presented in Figure 8.5. The differences between theory and measurement for the thicker wall cylinder is due to the skin effect, limiting the eddy currents to the skin depth and increasing the loop resistances, decreasing the time constants.

4. Non-Permeable Spheres: The properties of spheres are of interest both because the response can be analytically calculated (at least for non-ferrous metals) and because they are used as calibration targets for airport metal detectors. Figures 8.6 and 8.7 present the magnetic polarizability step responses for one and two inch diameter spheres machined from aluminum, brass, lead, and 304 stainless steel. The conductivities listed were adjusted to give the fits to the data shown; they are not the same for the two data sets because the spheres were not machined from the same pieces of stock. With this caveat about the conductivities, the data show excellent agreement with the theory of (III.81) and (III.82).

Figure 8.8 is the measured and analytical responses of some 1.5 inch diameter balls used for characterization of airport metal detector archways. These machined balls are not perfect spheres, so the decay curves deviate from theory more than the previous set of data.

Equation (III.81) is seen to describe the measured responses of non-ferrous spheres. The observed peak amplitudes of [1.2 , 0.5 , 0.15] are directly proportional to the diameters [2 , 1.5 , 1] cubed. The series expansion of (III.82) with both the amplitudes and time constants of the terms decreasing as $1/n^2$ is also observed.

5. Highly Permeable Spheres: The decay curves for highly permeable objects are not presently calculable. The formulation developed in Chapter 6 and summarized above makes the assumption that the permeability is a constant. In actuality, the permeability is a very non-linear function of several factors, including the strength of the incident magnetic field and the frequency components of the field and induced currents (it changes with time during and after the impulse excitation). It is also a non-linear function of temperature, past magnetic history (hysteresis), and several other factors.

The data presented in Figures 8.9 and 8.10 for magnetic spheres and balls are typical for magnetic materials. The step response polarizability has an initial fast rise from baseline (here shown as a negative excursion), followed by a much slower decay back to baseline. The response can be modeled as a series of exponential decay terms, with the slower decay terms having coefficients of opposite sign than those of the faster terms. Note that this is not in agreement with (III.80) in which all of the terms have coefficients of the same sign. The data could be represented by the theory better if the second term in the denominator had its sign reversed. In fact, an empirical model, with one or two fast exponentials of negative amplitude coefficients and one or two slow exponentials of positive amplitude, fits the observed data reasonably well.

The data curves cluster according to the size of the spheres. The composition of the magnetic material has only a minor effect on the response. These differences are probably due to the differences in the conductivities, as it is noted that the curves with the slower rises are the carbon steel balls. The faster rises of the stainless steel objects are indicative of the lower conductivities of these materials. The amplitudes are again observed to scale as the cubic power of the radius.

400-series stainless steel exhibits high-permeability magnetic properties, as opposed to the non-magnetic response of the 300-series stainless steel shown earlier. This is important for weapons detection because only the 400-series is hard and strong enough to use in manufacture of knives and guns. Hence, such weapons always show a strong magnetic response, virtually indistinguishable from that of ordinary hard steel.

6. Thin Disks: Data were taken for aluminum disks of two and four inch diameters, from sheet stock of nominal thicknesses 1/4", 1/8", 1/16", 1/32", and .020". The deconvolved responses are shown in Figures 8.11 and 8.12. For disk radius a and thickness h, an empirical fit is derived to fit the data:

$$S(t) \approx -20\,\pi\,a^3 \sum_{\alpha=1}^{\infty} \frac{e^{-t/\tau_n}}{n^3\,\pi^2}\,u(t)\ , \qquad \text{(IV.1)}$$

with:

$$\tau_n \approx \frac{a\,h\,\mu\,\sigma}{9\,n^2}\ , \qquad \text{(IV.2)}$$

The disks were machined from different sheets of aluminum of different alloys and unknown conductivities. The values presented are such as to make the theory fit the data. The fundamental time constant τ_1 certainly is proportional to the product of the thickness and radius.

7. Solid Cylinders: Data for one inch diameter by one inch high solid right circular cylinders are shown in Figure 8.13 for incident magnetic field parallel to the cylinder axis. Again, an empirical fit is derived to fit the data:

$$S(t) \approx -50\,a^3 \sum_{\alpha=1}^{\infty} \frac{e^{-t/\tau_n}}{n^2\,\pi^2}\,u(t)\ , \qquad \text{(IV.3)}$$

with:

$$\tau_n \approx \frac{a\,h\,\mu\,\sigma}{18\,n^2} \,. \qquad \text{(IV.4)}$$

The amplitudes are larger than those of the spherical formula (50 *vs* 12π), as are the time constants ($ah/18$ *vs* a^2/π^2), consistent with the 50% larger volume ($\pi a^2 h = 2\pi a^3$ *vs* $4\pi a^3/3$) of the cylinders, with $h=2a$.

V. CONCLUSIONS

The theory of magnetic singularity identification is shown to be in excellent agreement with measured data for non-ferromagnetic canonical objects.

The theory for ferrous objects is incomplete. The early time behavior resembles that of non-ferrous materials with high frequency components in the regime where permeability decreases to that of free space. Late time behavior is characterized by decay terms with opposite amplitude of the early time terms, which is not shown by (III.78) or (III.80).

Eddy currents are induced in non-ferrous conductors which circulate in such a direction as to produce fields that oppose (cancel) the incident field, which is a manifestation of Lenz's law. Amperian currents induced in ferrous material, however, produce fields that enhance the incident field, which is why soft iron is used in armatures and field windings of electric motors. Note the distinction between eddy currents and Amperian currents by the repulsion of a good conductor from an oscillating electromagnet, which attracts iron or steel. This opposite polarity of eddy currents *vs* Amperian currents [7] results in the negative polarity of the ferrous object signatures. It can also give the interesting results of a thin steel object, which exhibits a non-ferrous response when the incident magnetic field is normal to its surface and a ferrous response when it is aligned parallel to the surface. In the first case, the eddy currents induced in the large surface area dominate the amperian currents induced in the thin thickness. In the second case, the surface area for the eddy currents is very small compared to the long dimension in which the amperian currents are induced, so the latter dominate the response.

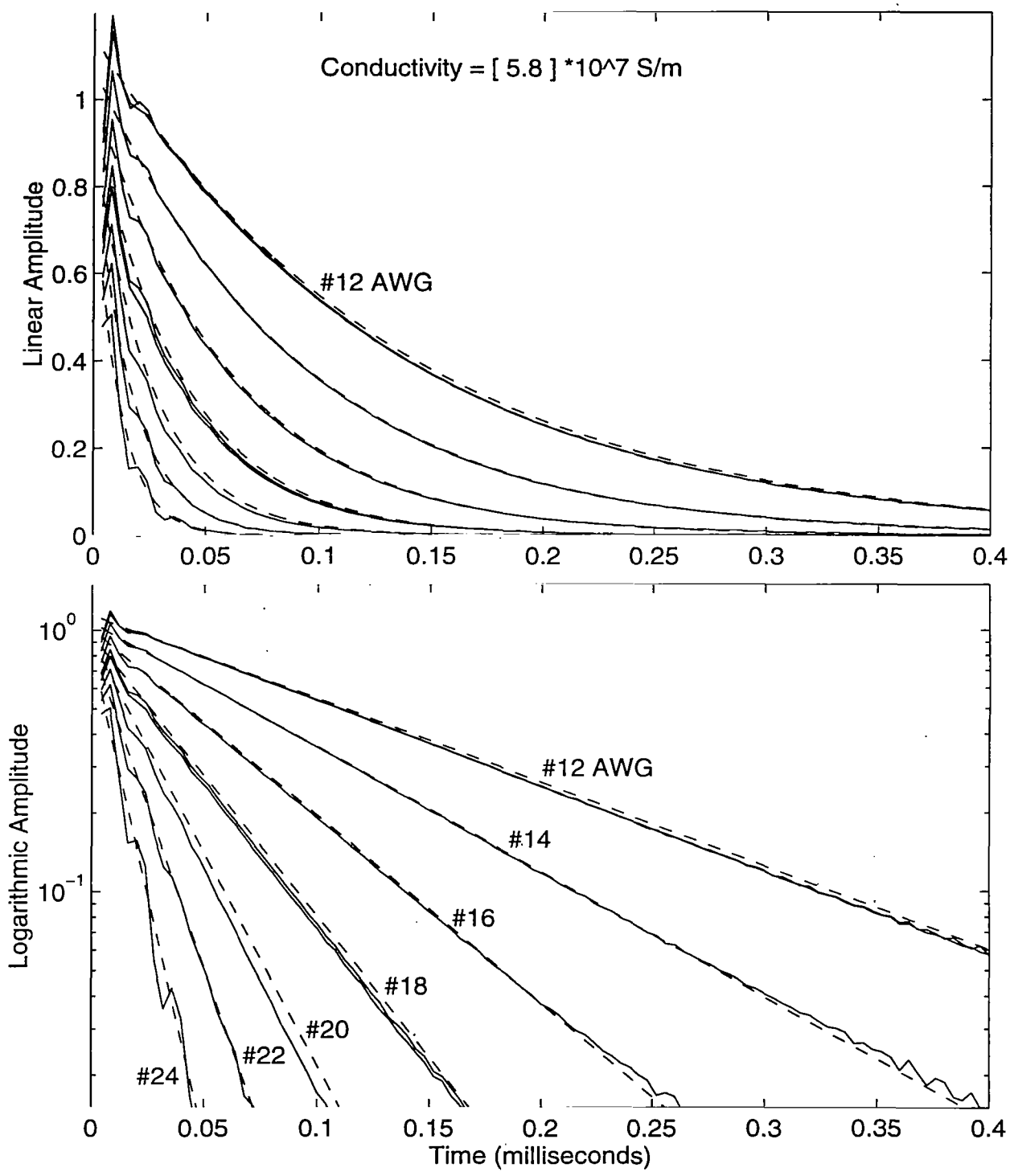

Figure 8.2. 5 cm Diameter Magnet Wire Loops: #12, #14, #16, #18, #20, #22, #24 AWG

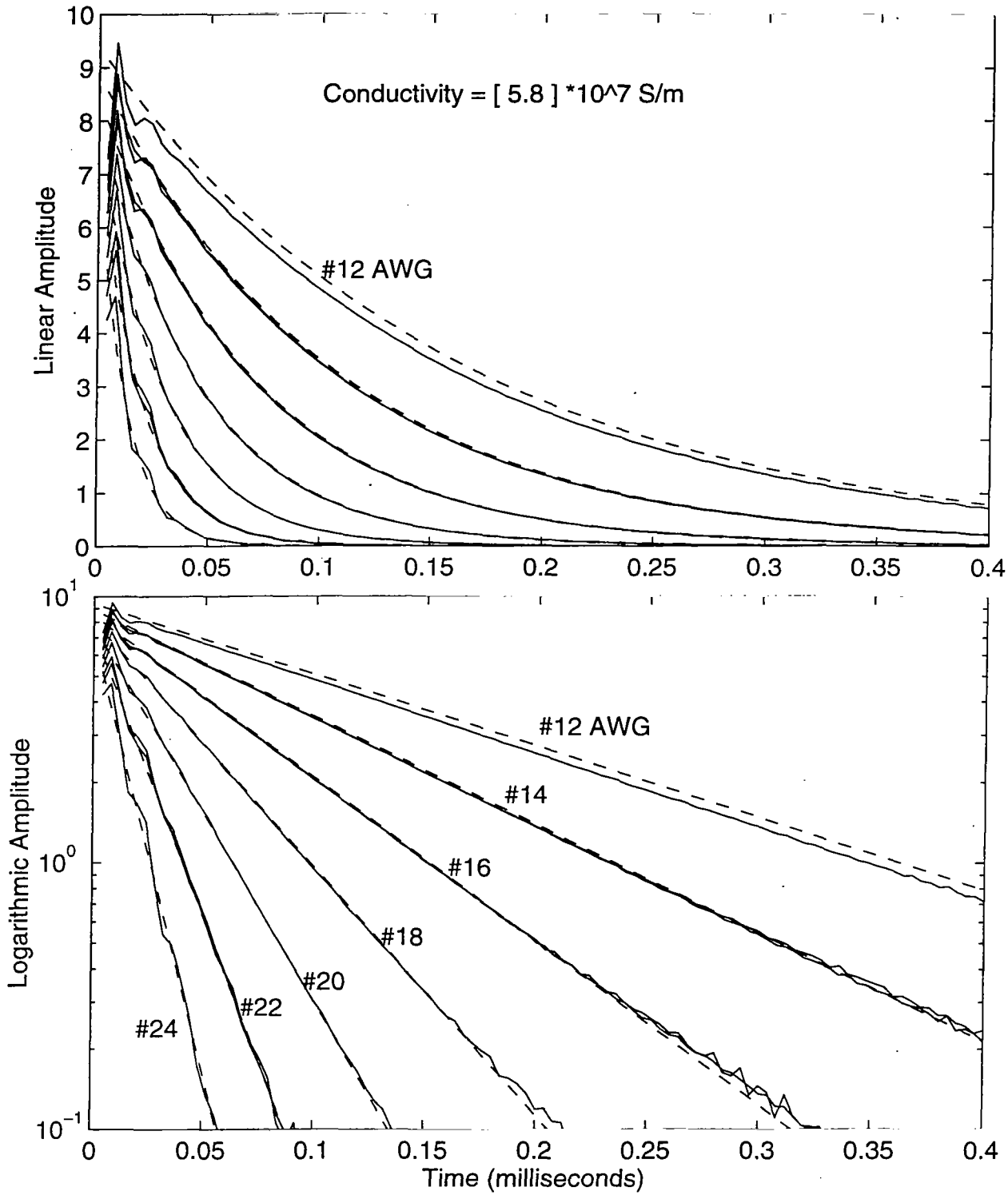

Figure 8.3. 10 cm Diameter Magnet Wire Loops: #12, #14, #16, #18, #20, #22, #24 AWG

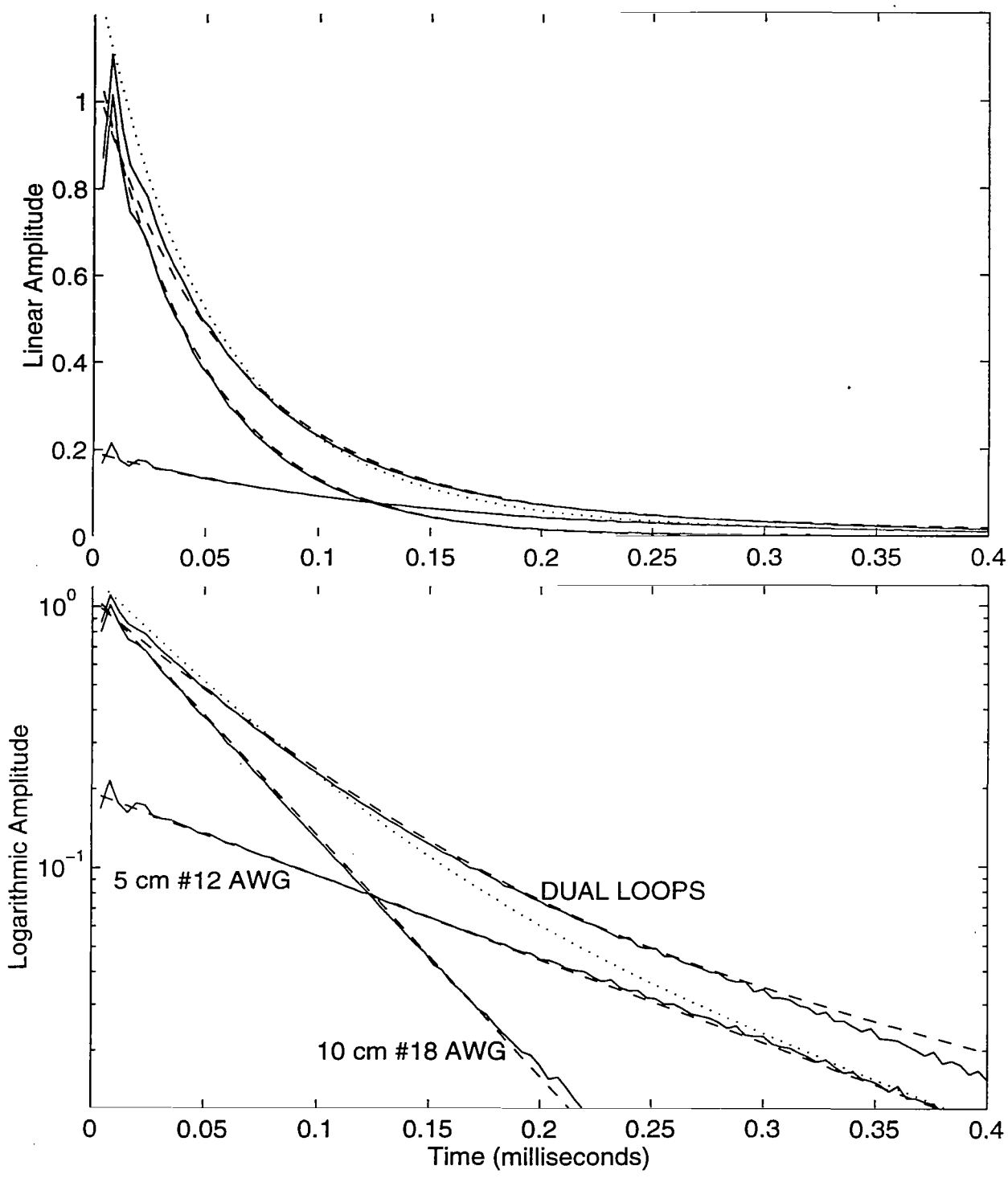

Figure 8.4. Dual Magnet Wire Loops: 5 cm #12 AWG and 10 cm #18 AWG.

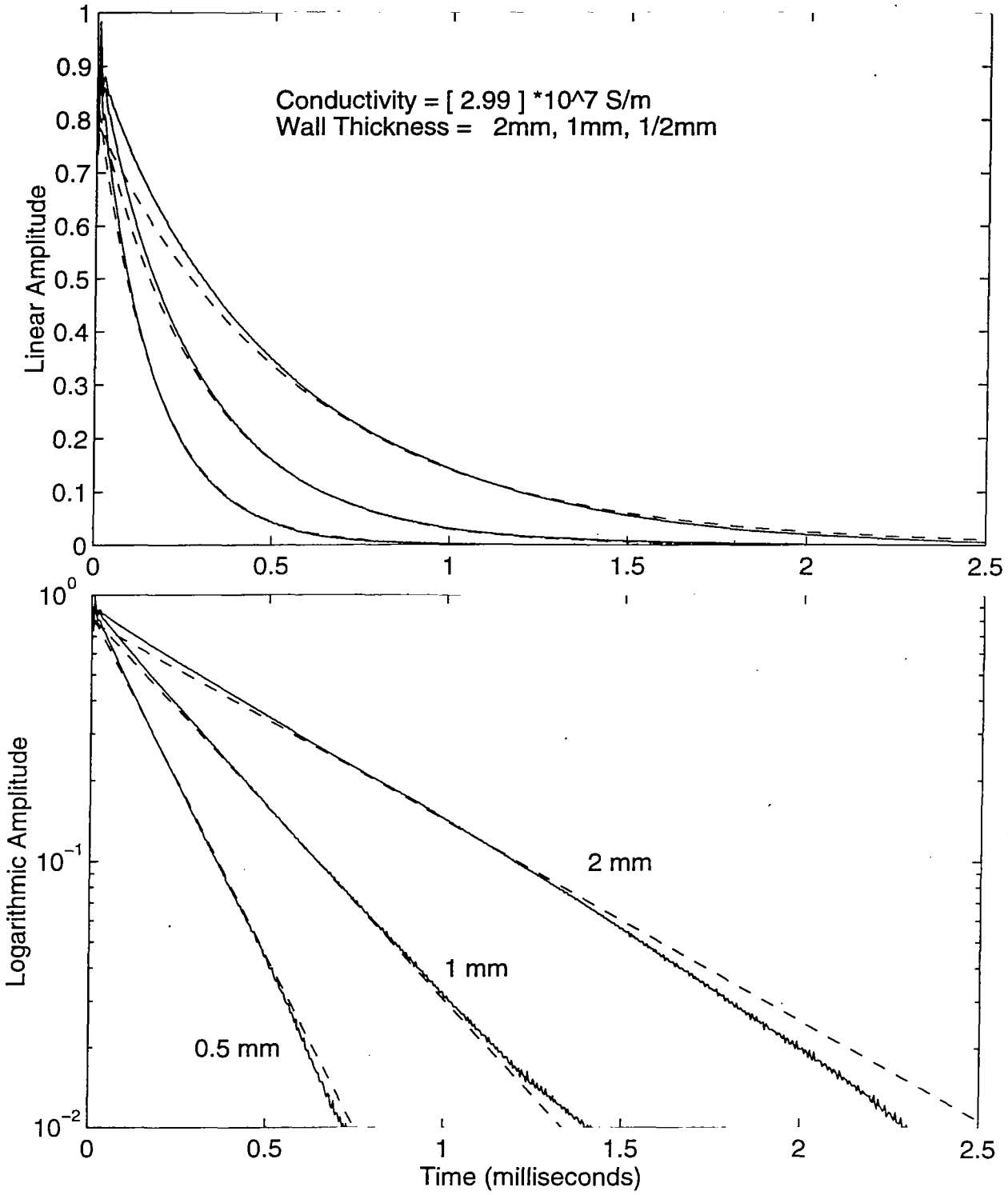

Figure 8.5. 5 cm Diameter by 5.5 cm Long Hollow Aluminum Cylinders.

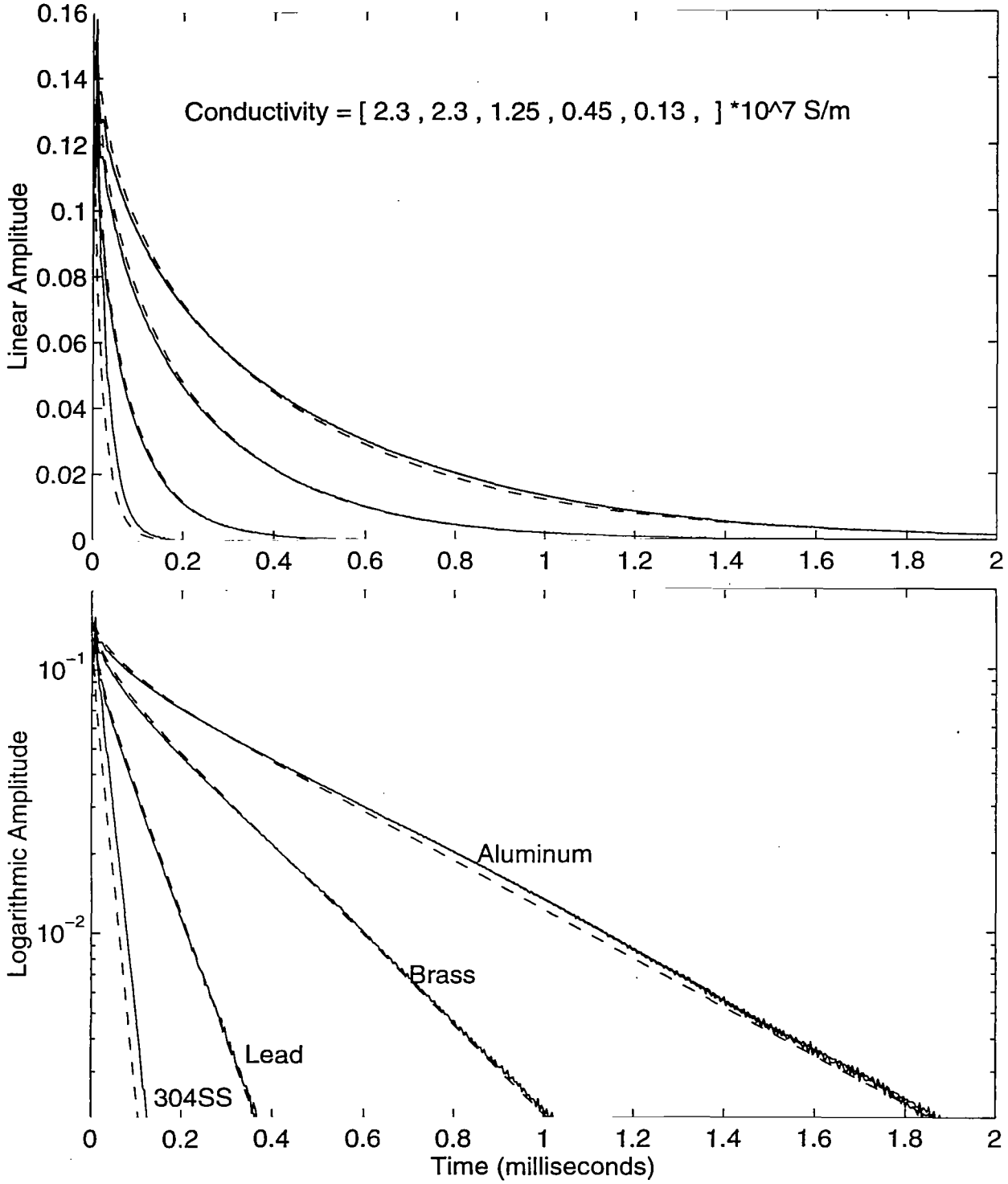

Figure 8.6. 1.00 Inch Diameter Spheres: Aluminum, Brass, Lead, 304 Stainless.

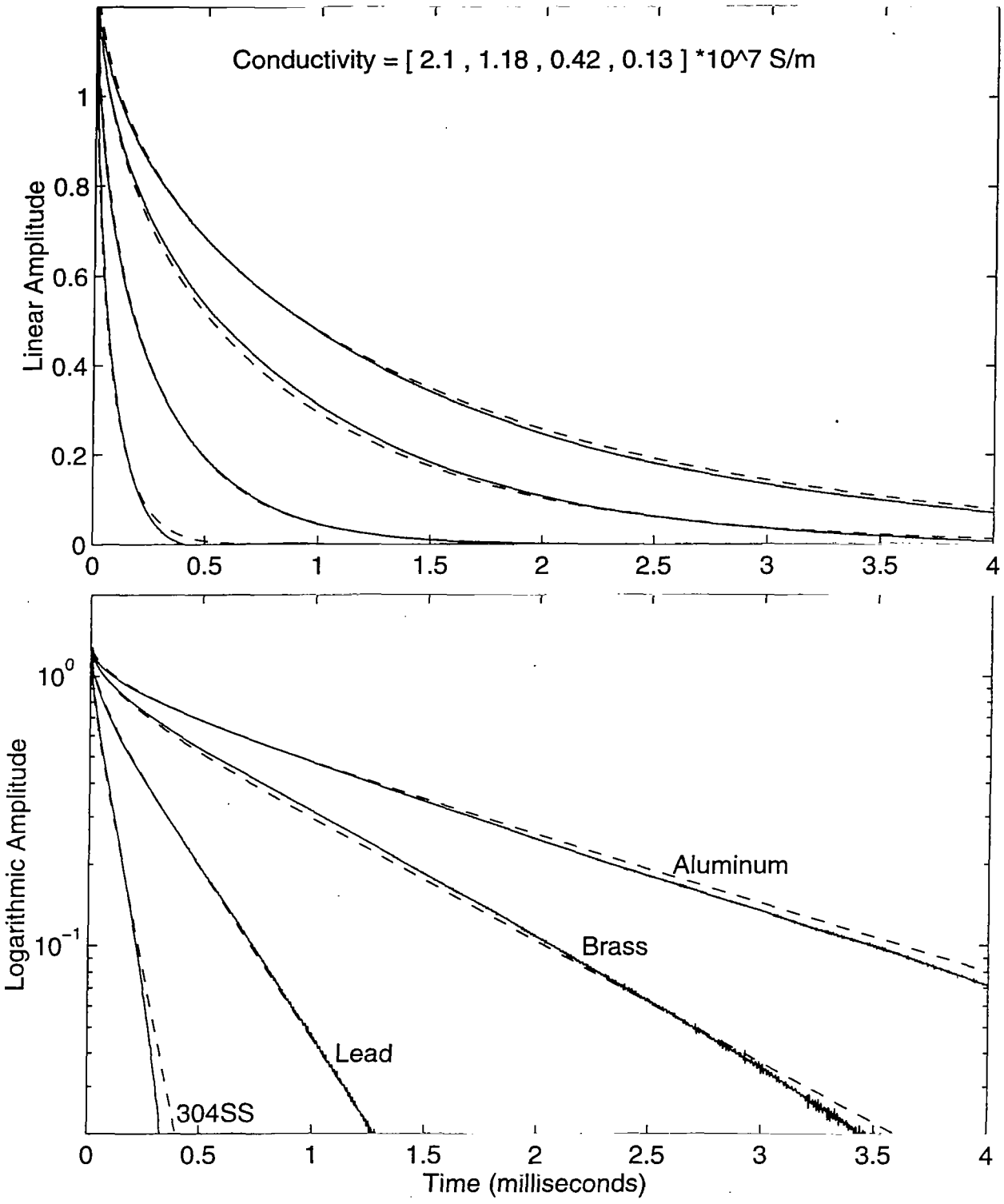

Figure 8.7. 2.00 Inch Diameter Spheres: Aluminum, Brass, Lead, 304 Stainless.

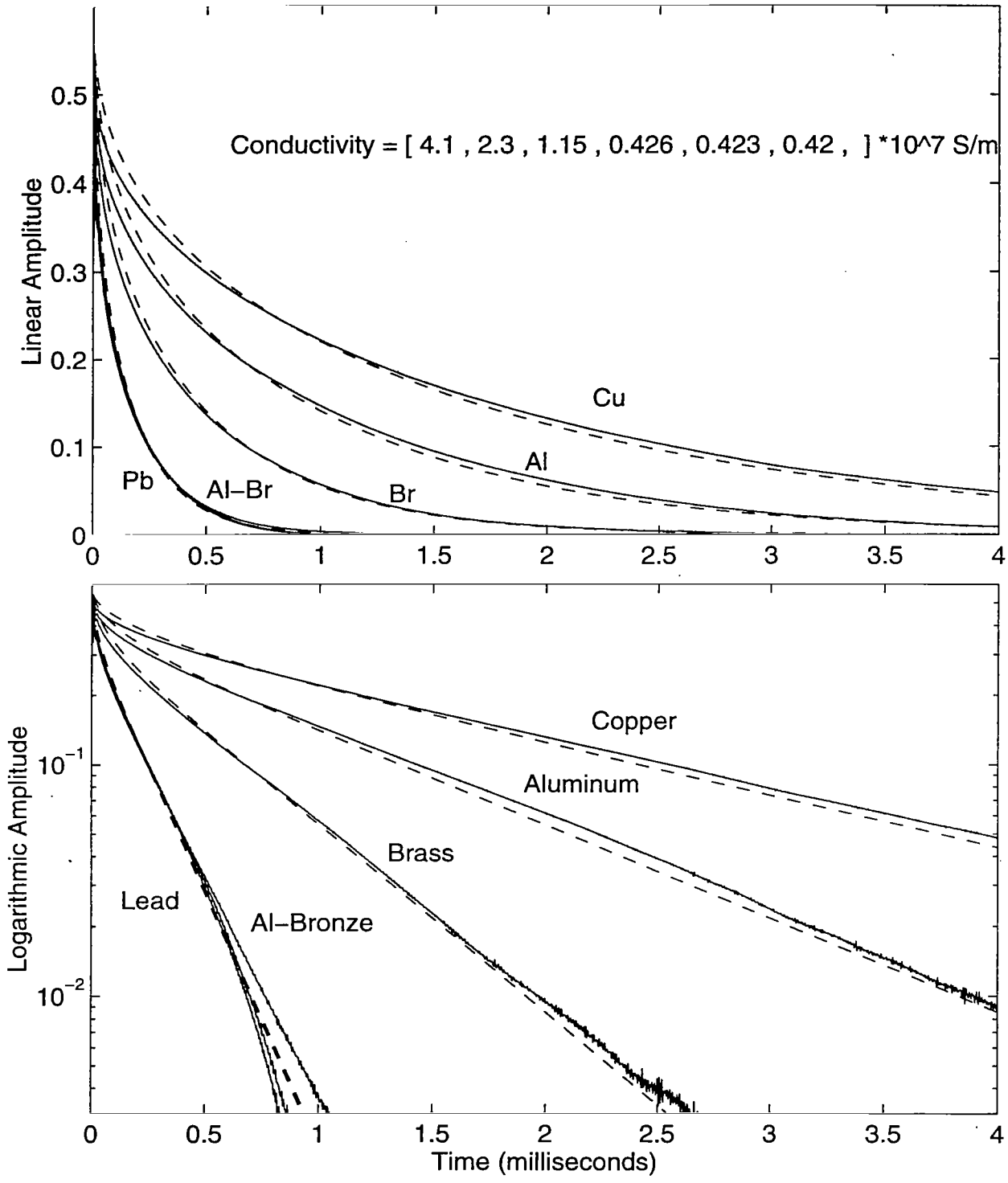

Figure 8.8. 1.50 Inch Diameter Balls: Copper, Aluminum, Brass, Zinc, Aluminum Bronze, Lead.

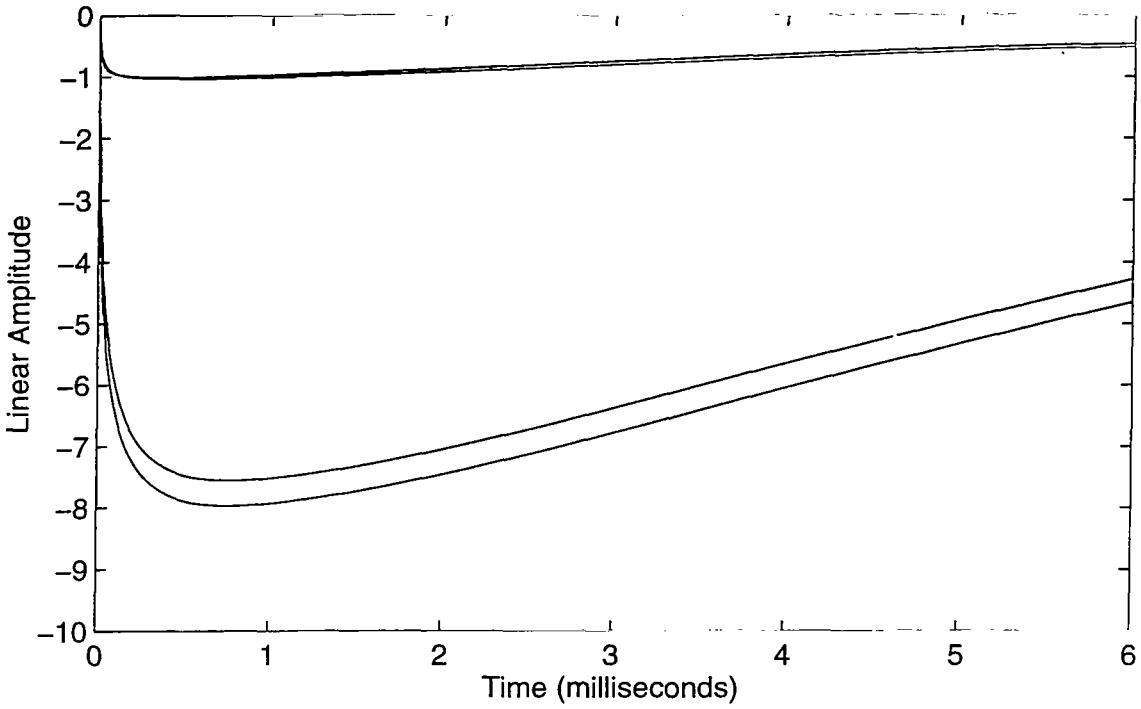

Figure 8.9. Magnetic Balls: One and Two Inch Diameter Chrome Steel, 440 Stainless.

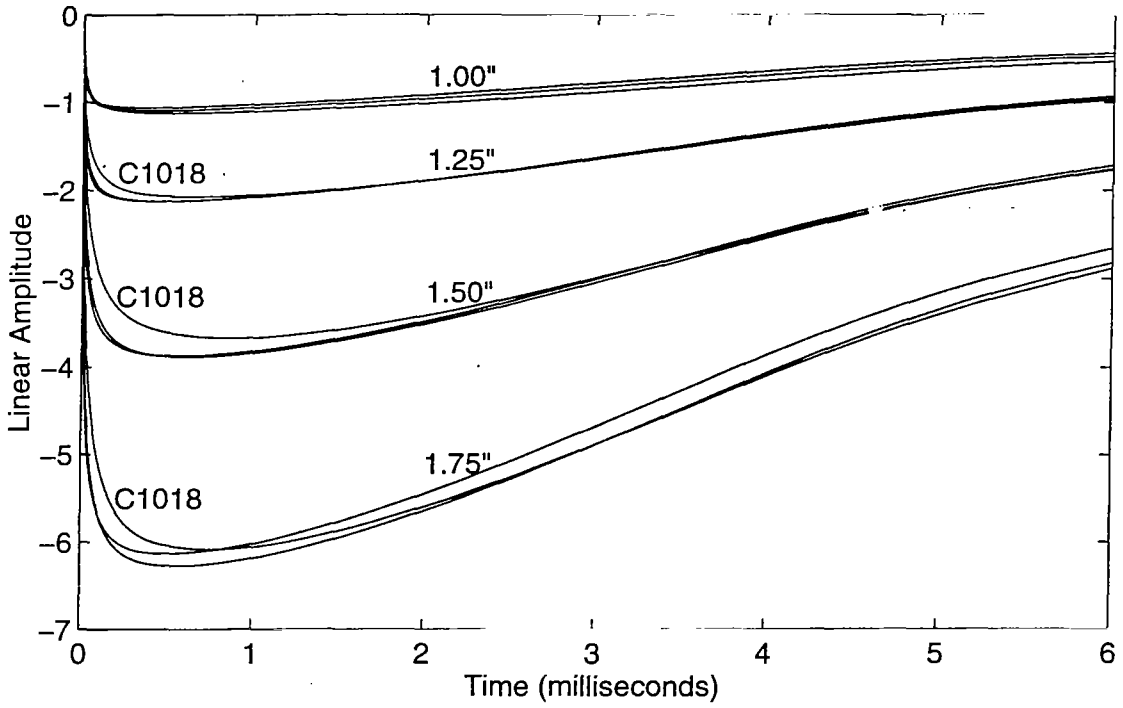

Figure 8.10. Magnetic Balls: 1.75, 1.50, 1.25, 1.00 Inch Diameters;
1018 Carbon Steel, 440 Stainless, 174 Stainless.

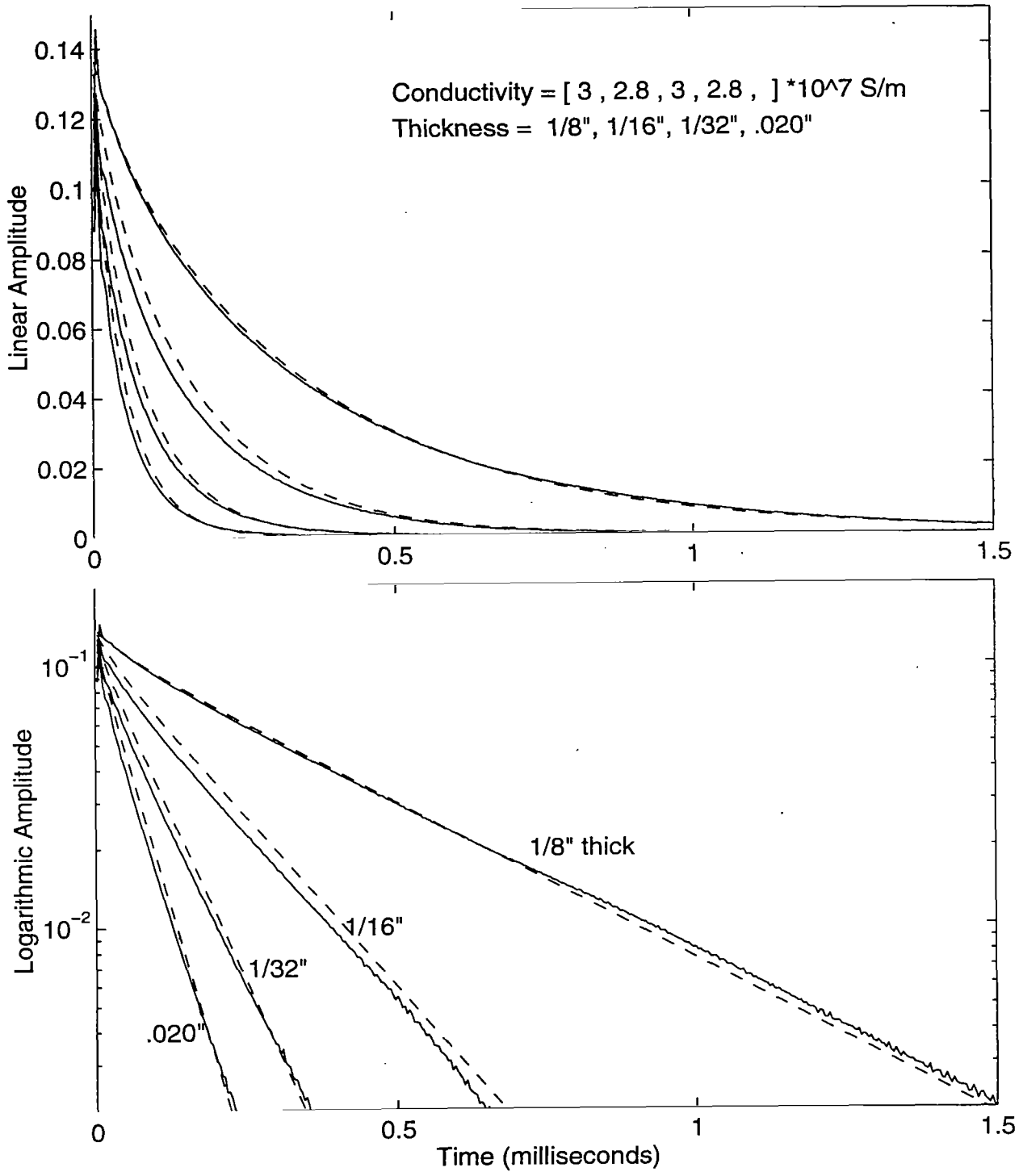

Figure 8.11. 5 cm Diameter Aluminum Disks.

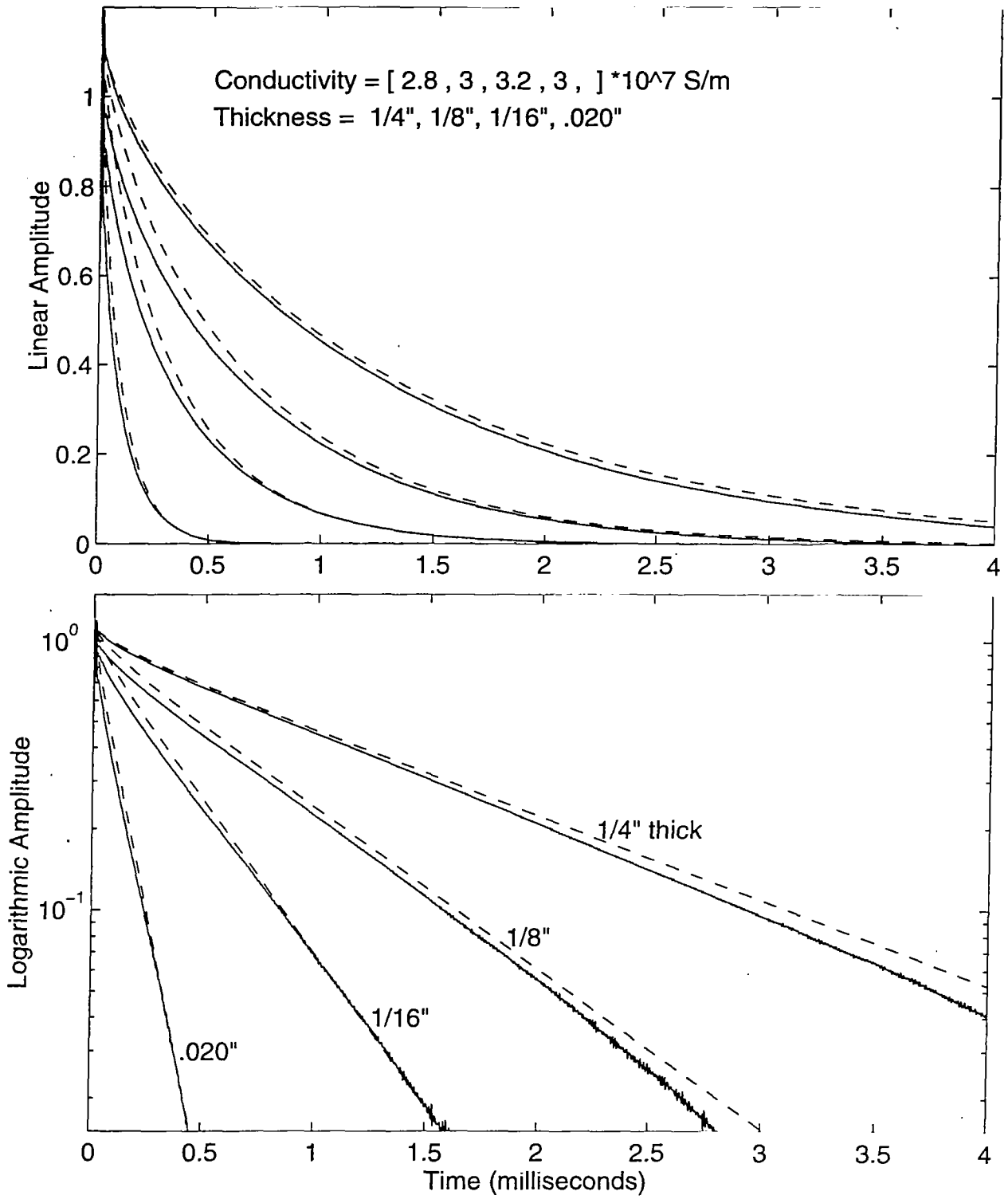

Figure 8.12. 10 cm Diameter Aluminum Disks.

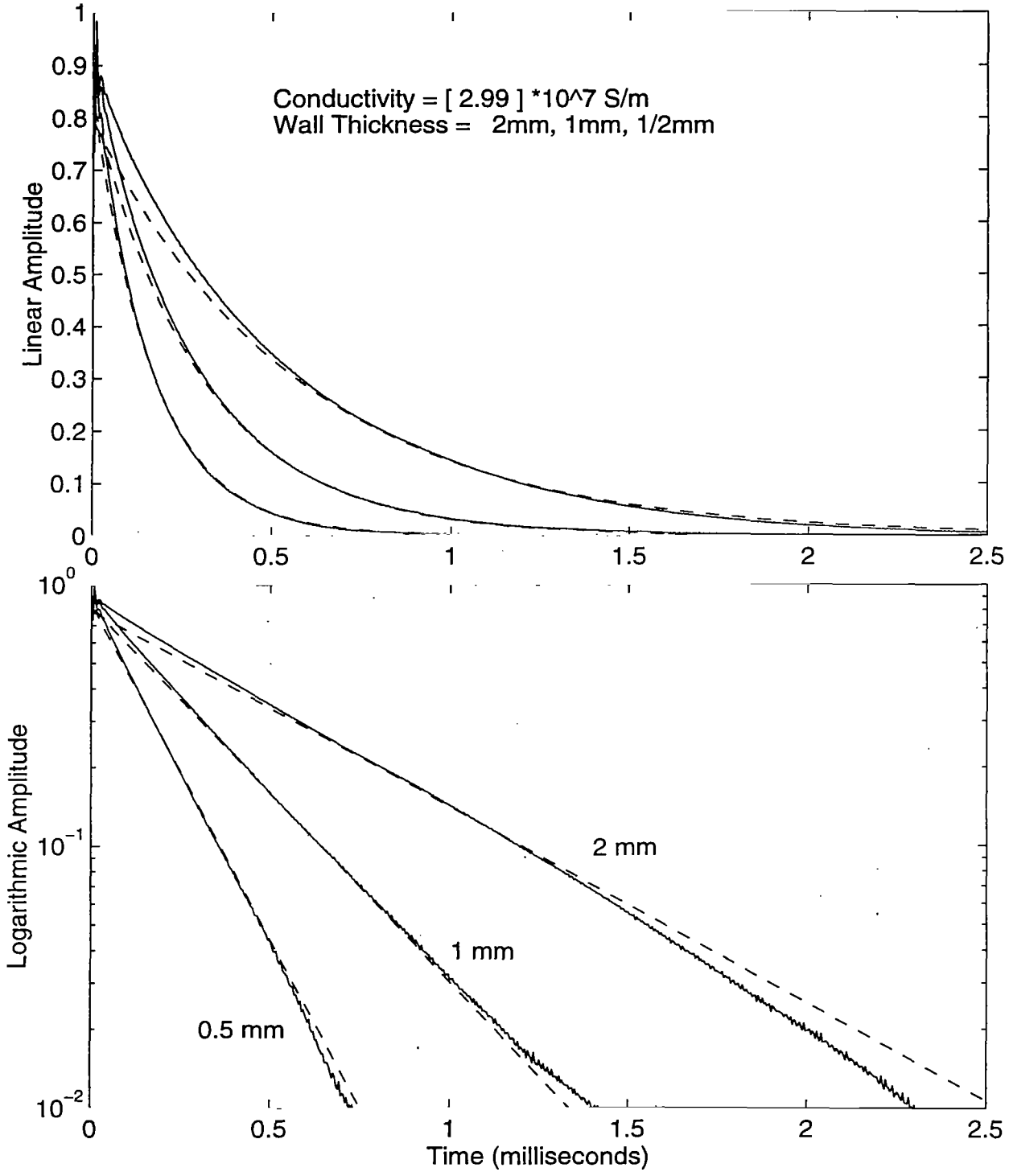

Figure 8.13. 1.00 Inch Diameter by 1.00 Inch Long Solid Cylinders.

REFERENCES

1. C. E. Baum, "Low-Frequency Near-Field Magnetic Scattering from Highly, but not Perfectly, Conducting Bodies," Interaction Note 499, Phillips Laboratory, 24 November, 1993.

2. F. W. Grover, Inductance Calculations: Working Formulas and Tables, Dover, New York NY, 1946.

3. S. Ramo, J. R. Whinnery and T. Van Duzer, Fields and Waves in Communication Electronics, J. Wiley and Sons, New York, 1965.

4. American Institute of Physics Handbook, McGraw-Hill, New York, 1963.

5. W. R. Smythe, Static and Dynamic Electricity, Mcgraw-Hill, New York, 1950.

6. D. R. J. White, Electromagnetic Shielding - Materials and Performance, Don White Consultants, Inc., Gainsville, VA, 1980.

7. W. M. Saslow, "How a Superconductor Supports a Magnet, How Magnetically "Soft" Iron Attracts a Magnet, and Eddy Currents for the Uninitiated," Am. J. Phys. 59, January 1991.